Transmission Bandwidth Enhancement Using Lateral Displacement in a Thin Flexible Single Layer Double Sided FSS.

Aliya A. Dewani, Steven G. O'Keefe, David V. Thiel

Griffith School of Engineering, Griffith University, Brisbane, Qld, Australia

***Abstract*— A novel low profile frequency selective surfaces (FSS) with wide stop band characteristics suitable for UWB applications consists of square loops screen printed on both sides of a thin flexible polycarbonate substrate with a lateral offset in both directions. The design provides a -10dB insertion bandwidth of 4.55 - 12.77GHz. The design delivers stop band for angular incidence in both single sided and double sided configurations up to 60° degrees. The symmetrical nature ensures identical response for TE and TM modes of polarization within 30° incidence. A comprehensive iterative analysis was made to enhance the ultra-wide bandwidth.**

Keywords—Frequency selective surfaces; lateral displacement; ultra-wide band; bandwidth enhancement.

I. INTRODUCTION

Frequency selective surfaces are planar periodic structures arranged in a one or two dimensional lattice printed on a dielectric substrate. The frequency selective surface can filter electromagnetic energy i.e. transparent to electromagnetic waves at certain frequencies and reflective/absorptive at others. Frequency selective surfaces have found enormous applications in microwave and optical systems. These periodic structures have been used as polarizers, filters, sub reflectors, radomes in order to control the radar cross section of the antenna configuration **[1].** Some FSSs also offer the advantages of flexibility, optical transparency, thinness and enhanced bandwidth **[2].** Different element geometries and dielectric substrates can enhance the bandwidth of an antenna system. The gain of the ultra-wideband antenna can be improved using a multilayer FSS **[3]** and in **[4]** the authors have introduced a wideband FSS by combining different resonating elements. However the stacked multilayers make the structure thicker, less mechanically flexible and less transparent. Fractals known for unit cell size reduction have been used for multiband FSS **[5]**. Comparatively large bandwidths have been achieved in intricate fractal designs, maintaining the compact FSS unit cell size **[6]**. From a design perspective, many other complex structures with different specifications have been used to improve the bandwidth including magnetic absorbers **[7],** space filling curves **[8]** and high impedance surfaces **[9].** In all cases, the filtering capacity is improved whereas the shielding bandwidth is narrow. In order to address the issue of design complexity, a simple compact size FSS is desired which can ensure the performance with varying angles of incidence and can provide an ultra-wide stop band.

This paper presents a double sided FSS that exhibits a -10 dB stop bandwidth of 8.22GHz ranging from 4.55 - 12.77GHz. We propose a single layer FSS printed on each side of a thin flexible dielectric substrate. The FSS elements are an array of square loops on the top side and an identical array displaced on the bottom side of the dielectric substrate. The displacement changes the resonant frequency of the metallic loops and the bandwidth can be increased two fold. The dimensions of the FSS elements are much smaller ($\lambda_o/5$) than the operating wavelength. Section II represents the FSS geometry, design specifications and the various offset techniques used for bandwidth enhancement. The transmission response and angular stability of the FSS structure are discussed in section III. Various parameters and their effect on the FSS performance are dealt with in section IV. The FSS design has the advantages of a less complex structure, enhanced bandwidth due to half period displacements in the two directions, angular stability, polarization insensitivity and easy mass production in sheets.

II. FSS DESIGN AND SPECIFICATIONS

Fig. 1. shows the layout and the respective cross section of the basic model. The FSS structure consists of two printed metallic layers on both sides of the dielectric substrate. The pattern consists of a regular array of square loops and the supporting dielectric substrate is a flexible thin transparent film of polycarbonate, with relative permittivity 3.2, loss tangent 0.0025 and thickness, h = 0.21mm.

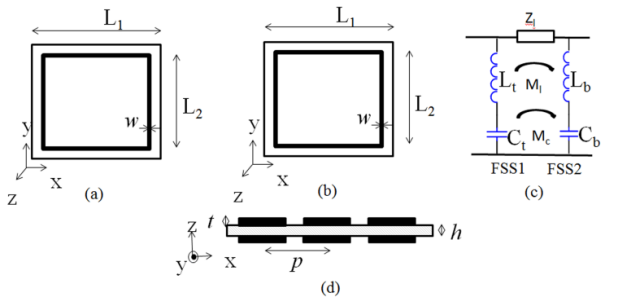

Fig. 1. Double sided Square Loop Stop band FSS unit cell. (a) FSS- Top side. (b) FSS- Bottom side. c) Equivalent circuit showing inductance and capacitance associated with the double sided square loop. (d) Cross-sectional side view from x-z plane.

In modelling investigation the FSS structure is assumed to be an infinite periodic structure. The FSS is illuminated by a plane wave, with electric field vector E oriented in y direction and the magnetic field vector H oriented in x-direction. The FSS structure behaves like a series LC resonator where the loop contributes to inductance and the gap in between the two adjacent elements provides the capacitance **[2]**. The mutual coupling between the two sides is modelled as mutual inductance and capacitance. Since the thickness of the substrate is small, its equivalent transmission line length can be neglected. Therefore, the equivalent circuit is simplified as a parallel circuit of top series (FSS1) and bottom series (FSS2) LC resonators (Fig.1). The values of mutual capacitance, M_c and mutual inductance, M_l depend on the overlap of the metallic tracks and will vary in different configurations. The transmission is blocked by this FSS structure at its resonant frequency, therefore behaving as a stop band filter. The performance of the FSS was calculated using CST microwave studio, which uses full wave methods of simulation. The unit cell boundary conditions are set in the directions of periodicity.

A. FSS Layer Offset

The enhancement of bandwidth is achieved due to lateral displacement of the bottom side relative to the top. The relative lateral displacement is important in the electromagnetic design as it involves a change in the mutual inductance and capacitance of the conducting elements. In this paper, various offset techniques were used to implement shifts in the stopband frequency while maintaining the compactness of the unit cell. In the numerical model the top side was fixed and the bottom was shifted in *x* and *y* direction as shown in Fig. 2 and 3.

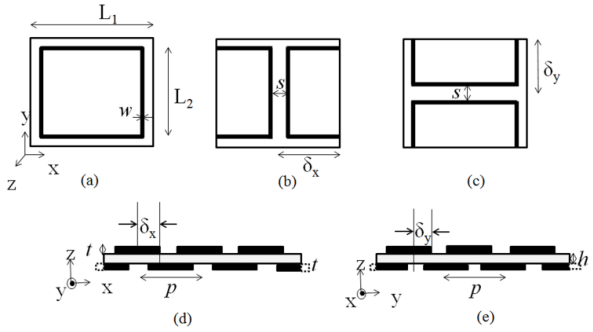

Fig. 2. Double sided square loop stop band FSS unit cell with half period displacement in x- or y- axis. (a) FSS top side. (b) FSS bottom side.- displaced in x-direction. (c) FSS bottom side.- displaced in y-direction. (d) Cross sectional view from x-z plane, $\delta_x = 0.5L_1$. (e) Cross sectional side view from y-z plane, $\delta_y = 0.5L_1$.

Shifting the square loop on the bottom side of the dielectric by a half cell in x-axis ($\delta x = 0.5L_1$) or in y-axis ($\delta y = 0.5L_1$) does not affect the centre frequency of the stop band. However, the displacement parallel to incident E field (Y) leads to a slightly broader bandwidth as compared to the displacement parallel to the magnetic field (X). The half period offset was made in both *x* and *y* axes simultaneously, i.e. $\delta x = \delta y = 0.5L_1$ as shown in Fig. 3. Such an offset showed a wider bandwidth due to the increase in mutual inductance M_l and the mutual capacitance, M_c as compared to the other FSS configurations. The reason being that the lumped inductor and capacitor are placed in a way that they can have maximum coupling to the electric and magnetic field of the incident plane wave.

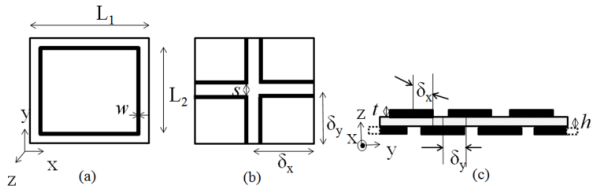

Fig. 3. Double sided square loop stop band FSS unit cell with half period displacement in *x* and *y* axis. (a) FSS top side. (b) FSS bottom side-displaced in *x*-and *y*- direction (d) Cross sectional side view from y-z plane, $\delta_x = 0.5L_1$ and $\delta_y = 0.5L_1$.

The dimensions of the structure used in this investigation are given in the Table 1.

Table 1. Physical dimensions of FSS square loop (see Fig. 2 and 3)

Parameters	***Description***	***Dimensions(mm)***
L_1	Unit cell size	8.00
L_2	Outer Sq. loop length	7.20
t	Thickness of track	0.01
s	Spacing in between loops	0.80
w	Width of Track	0.30
h	Thickness of Substrate	0.21

III. TRANSMISSION CHARACTERISTICS

A. Normal Incidence

The transmission response of the double sided FSS structure with the layer offset at normal incidence was analyzed (see Fig 4). The conductive tracks on both sides form the capacitive and inductive surfaces. As the FSS element was displaced on one side, opposite currents flow in the loop tracks increasing the mutual inductance and capacitance of the structure thereby shifting the stop band.

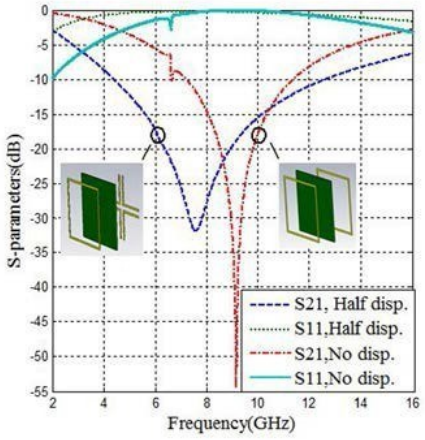

Fig. 4. Transmission and Reflection response of double sided square loop FSS The Red line (-.-) and Green line (solid) represent the transmission and reflection response for the displacement of $\delta x = \delta y = 0L_1$ .The response is for normal plane wave incidence with $L_1 = 8$mm, $L_2 = 7.2$ mm, $p = 8$ mm, $w = 0.3$ mm, $t = 0.01$ mm, $h = 0.21$mm.

Such displacements increase the bandwidth of the FSS. The simulated results show the maximum bandwidth was obtained by positioning the FSS such that the individual element sides of a bottom side lie at one half-cell apart in x and y direction to those of the top side when viewed from the normal angle of incidence. The results are given in Table 2.

Table 2: Transmission response of the double sided FSS with various configurations at normal wave incidence.

Substrate thickness, h	***Displacement***		***f_r* (GHz)**	**- 10dB BW(GHz)**
	Δx	***Δy***		
0.2mm	0	0	9.14	4.27
0.2mm	$0.5L_1$	0	14.18	9.00
0.2mm	0	$0.5L_1$	14.18	8.96
0.2mm	$0.5L_1$	$0.5L_1$	7.60	8.12

B. Angular sensitivity:

It is important that the FSS provides stable performance for various incident angles and different polarizations within its operating frequencies. In order to check the impact of incident angle, various incident angles (0^o, 15^o, 30^o, 45^o, 60^o) were carried out for TE and TM polarizations. The results are given in Fig.5.

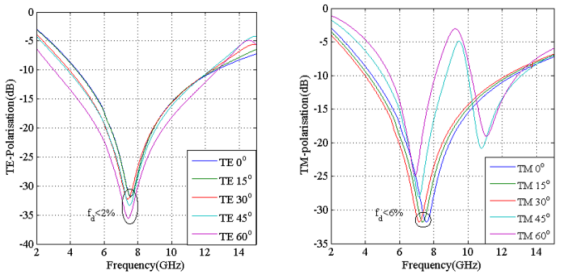

(a) (b)

Fig. 5. Transmission coefficients as a function of frequency for various incident angles. (a) TE polarization (b) TM polarization.

The double sided square loop FSS has a very small (less than 2%) change in resonant frequency for TE polarization compared to the TM polarization response. The general features of the stop band remains the same as that of the normal incidence for TE polarization. Fig. 5(a) shows a well-defined stop-band at 7.60GHz and the higher order resonances corresponding to higher angles appears unchanged. Fig. 5(b) shows the TM mode shifts by 6% (7.60GHz to 7.15GHz) within the 30^o angle of incidence. For TM polarization, at higher angles (e.g. 45^o, 60^o) apart from the resonant frequency which is 7.13GHz and 6.90GHz respectively (Fig 6), the grating lobes also appear at 10.80 GHz and 11 GHz. This explains that for higher angle of incidence the FSS shows angular sensitivity.

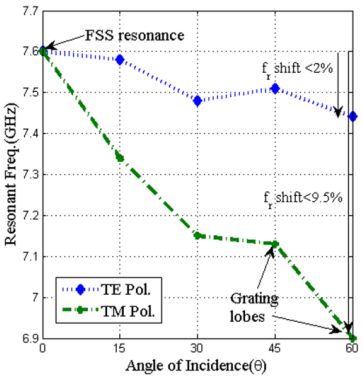

Fig. 6. The resonant frequency is a function of angle of incidence for TE and TM response. The grating lobes start to appear for angles greater than 30^o for TM polarization.

IV. BANDWIDTH

A. Substrate thickness:

The fundamental resonant frequency of the FSS is altered by changing the thickness of its supporting dielectric. With the increase in the thickness of the dielectric, the layer offset configurations show an initial decline of the resonant frequency from the free space value. The air/dielectric boundary is close to the conducting elements in this region. At the boundary, the low order evanescent Floquet modes decay exponentially with distance from the conducting elements. This modifies the relative amplitudes and the resonant frequency of the FSS with respect to the supporting dielectric layer **[10]**.

For half period displacement in either *x* or *y* directions, the structure resonates at a higher frequency of about 14.18GHz with a bandwidth of nearly 9GHz for 0.21mm dielectric thickness. For the same thickness and half period displacement in the *x* and *y* directions, the structure resonates at a slightly lower frequency of 7.60GHz with a bandwidth of nearly 8.20GHz. This means that the half-cell displacement increases the mutual inductance, M_l and slightly the mutual capacitance, M_c (Fig. 1c) which lowers the band stop frequency. Beyond the thickness of 2mm, there is a periodic wave drop and rise in bandwidth. The peaks in the bandwidth curve are due to the combined effect of dielectric loading effect on two sides of the plastic and the back reflections from the plastic for a given substrate thickness. This effect causes broadening/narrowing of the curve near/at the quarter and half wavelength thicknesses of the plastic substrate **[2]**.

B. Inter element spacing:

As the inter element spacing is increased, the mutual coupling decreases and this leads to grating lobes in the transmission curve which reduces the angular stability of the response. The mutual element coupling is unaffected by the change in the angle of incidence. Only the phase associated with the induced currents in the FSS elements change with angle of incidence **[11].**

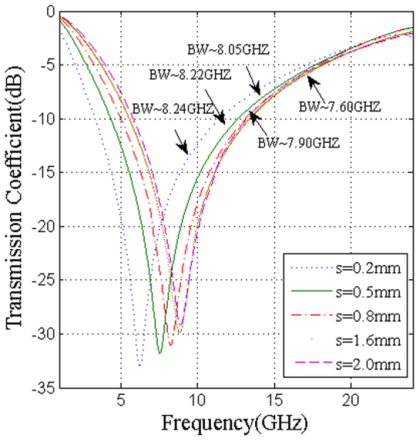

Fig. 7. Simulated transmission response for the double sided square loop FSS with *x* and *y* offset bottom side, for different values of spacing *s*, ε_r=3.2, L_1= 8mm, L_2=7.2mm, *p*=8mm, *w*=0.3mm, *t*=0.01mm, *h*=0.21mm, δ_x=0.05L_1 and δ_y=0.05L_1.

The square lattice elements were placed following the general formula given in **[12]**. For normal incidence, L_1/λ_o is less than 1. The plot in Fig. 7 shows that if the spacing is decreased to 0.2mm without changing the other parameters, the bandwidth is further enhanced by 2.3%. However, the printing tolerances need to be considered when designing any FSS structure. No grating lobes appear up to an inter element spacing of 2mm.

C. Track Width

Another geometrical parameter found to regulate the bandwidth of the FSS was the track width of the square loop(Fig. 8) where the circumference of the inner square loop changes, when all other parameters were unchanged. This is because the circumference for the flow of current is limited as the track width increases which lowers the inductance and shifts the frequency higher.

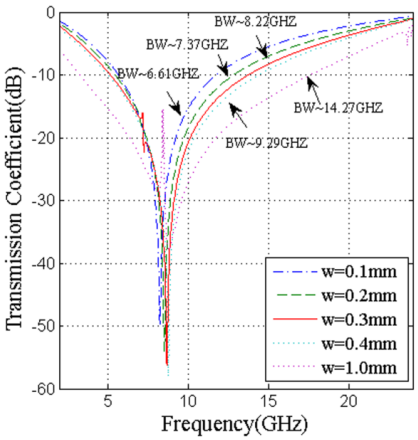

Fig. 8. Simulated transmission response for the double sided square loop FSS with *x* and *y* offset bottom side, for different values of track width '*w*'. As the loop size decrease the inductance increases, narrowing the bandwidth seen for a track width of 0.1mm the bandwidth is 6.61GHz.

V. CONCLUSION

In this paper, we have presented a novel low profile double sided FSS screen printed on a single layer of thin flexible and transparent substrate with lateral displacements on one of the sides. The -10dB bandwidth (4.55GHz to 12.77GHz) was found for a unit cell periodicity of λ_o/5. The transmission coefficient for different incident angles shows that the FSS is independent of small incident angles. The bandwidth can be reduced or enhanced by optimizing the three parameters of the structure: substrate thickness, inter element spacing and track width. Apart from the promising future applications in radomes, curved surfaces and other antenna applications, the FSS can provide frequency shielding over ultra-wide bands in hospitals where there is potential risk of interference between various operating systems like medical equipment and mobile phones existing in close proximity. Also the simple printed FSS geometry on a transparent substrate retains the optical and RF transparency for required applications.

REFERENCES

1. Y. Yang, X.-H, Wang, and H. Zhou, "Dual band frequency selective surface with minitaurised element in low frequencies", *Progress in Electromagnetic Research*, vol. 33, pp. 167-175, 2012.
2. A. A. Dewani, S. G. O'Keefe, D. V. Thiel and A. Galehdar, "Optically transparent frequency selective surfaces on flexible thin plastic substrate", *AIP Advances* ,vol 5, 027107, 2015.
3. Y. Ranga, L. Matekovits, K.P. Esselle and A. R. Weily,"Design and analysis of frequency selective surfaces for an ultra-wideband applications*", IEEE Int. Conf. on Computer as a Tool (EUROCON)*, Lisbon, 2011, pp.1-4.
4. Y. Ranga, L. Matekovits, K.P. Esselle and A. R. Weily, "Multilayer frequency selective surfaces reflector for constant gain over ultra-wideband",Proc of the 5th European conf. on Ant. and Propagat.(EUCAP), Rome, 2011, pp.332-334.
5. J. Romeu, and Y. Rahmat-Samii, "Fractal FSS: A novel dual band frequency selective surfaces", *IEEE Trans. Antennas Propag.*, vol. 45, pp. 1097-1105, 2000.
6. A. L. P. S Campos, E. E. C. Oliveira, and P. H. F. Silva, "Design of miniaturized frequency selective surfaces using Minkowski island fractal", *Journal of Microwaves, Optoelectronics and Electromagnetics applications*, vol.9, pp. 43-39, 2010.
7. N. I. Landy, S. Sajuyigbe, J. J. Mock, D. R. Smith, and W. J. Padilla, "Perfect Metamaterial Absorber", *Physical Review Letters*, vol.100, 207402, 2008.
8. D. Kim, J. Yeo, and J. Choi, "Broadband spatial band stop filter using Sierpenski space filling geometry at PCS band", *Microwave and Optical Tech. Lett.*, vol. 50, no.10, pp. 2716-2718, 2008.
9. O. Luukkonen, F. Costa, A. Monorchio, and S. A. Tretyakov, "A thin electromagnetic absorber for wide incidence and both polarizations", *IEEE Trans. Antennas Propag.*, vol. 57, pp. 3119- 3125, 2009.
10. P. Callaghan, E.A. Parker, and R. J. Langley, "Influence of supporting dielectric layers on the transmission properties of frequency selective surfaces", *IEE Proc. H*, vol. 138, pp. 448-454, 1991.
11. B. A. Munk, *Frequency selective surfaces: theory and design*. New York, NY, USA: Wiley, 2000.
12. J. Huang, T. K. Wu and S. W. Lee, "Triband frequency selective surfaces with circular ring elements", *IEEE Trans. Antennas Propag.* , vol.42, pp. 166-175, 1994.